Preprints (www.preprints.org) | NOT PEER-REVIEWED | Posted: 8 July 2019 doi:10.20944/preprints201907.0119.v1

Comparative mitochondrial genome analysis of the tobacco endophytic fungi *Leptosphaerulina chartarum* and *Curvularia trifolii* and the phylogenetic implications

Xiao-Long Yuan[a,#], Min Cao[b,#], Guo-Ming Shen[a], Huai-Bao Zhang[a], Yong-Mei Du[a], Zhong-Feng Zhang[a], Qian Li[c], Jia-Ming Gao[d], Lin Xue[e], Peng Zhang[a,*]

[a] Tobacco Research Institute of Chinese Academy of Agricultural Sciences, Qingdao, Shandong Province, China; rayrock@126.com (X.-L.Y.); shenguoming@caas.cn(G.-M. S.); zhanghuaibao@caas.cn (H.-B.Z); duyongmei@caas.cn (Y.-M.D.); zhangzhongfeng@caas.cn (Z.-F.Z.)[b] Marine Science and Engineering College, Qingdao Agricultural University, Qingdao, Shandong Province, China; caominjiayou@163.com(M.C.)

[c] Nanyang Tobacco Group Co., Ltd, Nanyang , Henan Province, China; qianqingzi@qq.com (Q.L.)

[d] Hubei Provincial Tobacco Company of China National Tobacco Corporation, Wuhan, Hubei Province, China; gaojiaming373@163.com (J.-M.G.)

[e] WannanTobacco Group Co., Ltd, Xuancheng, Anhui Province, China 893981088@qq.com (L.X.)

[#]These two authors contributed equally to this study.

Correspondence: ; zhangpeng@caas.cn (P.Z)

© 2019 by the author(s). Distributed under a Creative Commons CC BY license.

Preprints (www.preprints.org) | NOT PEER-REVIEWED | Posted: 8 July 2019 doi:10.20944/preprints201907.0119.v1

Preprints (www.preprints.org) | NOT PEER-REVIEWED | Posted: 8 July 2019 doi:10.20944/preprints201907.0119.v1

Abstract: In tobacco plants, symbiont endophytic fungi are widely distributed in all tissues where they play important roles. It is therefore important to determine the species distribution and characteristics of endophytic fungi in tobacco. Here, two parasitic fungi *Leptosphaerulina chartarum* and *Curvularia trifolii* were isolated and identified from normal tobacco tissue. We sequenced the mitogenomes of these two species and analysed their features, gene content, and evolutionary histories. The *L. chartarum* and *C. trifolii* mitochondrial genomes were 68,926 bp and 59,100 bp long circular molecules with average GC contents of 28.60% and 29.31%, respectively. The *L. chartarum* mitogenome contained 36 protein coding genes, 26 tRNA genes, and 2 rRNA genes (rrnL and rrnS), which were located on both strands. The *C. trifolii* mitogenome contained 26 protein coding genes, 29 tRNA genes, and 2 rRNA genes (rrnL and rrnS). The *L. chartarum* 26 tRNAs ranged from 70 bp to 84 bp in length, whereas the 29 tRNAs in *C. trifolii* ranged from 71 bp to 85 bp. *L. chartarum* and *C. trifolii* mtDNAs had an identical mitochondrial gene order and orientation and were phylogenetically identified as sisters. These data therefore provide an understanding of the gene content and evolutionary history of species within Pleosporales.

Key words: Endophytic fungi, *Leptosphaerulina chartarum*; *Curvularia trifolii*; mitogenomes; gene content; phylogenetic implications.

Preprints (www.preprints.org) | NOT PEER-REVIEWED | Posted: 8 July 2019 doi:10.20944/preprints201907.0119.v1

1. Introduction

Studies examining fungal endophytes in tobacco have shown that they are widely distributed in almost all tissues and due to their various biological functions they play very important roles in tobacco biology [1-3]. It is therefore important to determine the distribution of endophytic fungi species and their characteristics in tobacco. Pleosporales, the largest order in the fungal class Dothideomycetes, includes a large number of species, including saprobes, parasites, epiphytes, and endophytes [4]. Numerous reports have shown that many species in Pleosporales are pathogenic fungi that can cause severe disease that have an economically and culturally adverse effect on the global breeding industry and animal husbandry. Previous studies have shown that many endophytic fungi that belong to the Pleosporales order can be isolated from the healthy tissues of tobacco (*Nicotiana tabacum*) [5]. The family Pleosporaceae includes a variety of species that are plant pathogens, animal parasites, and saprotrophs. Two particularly important parasitic species are *Leptosphaerulina chartarum*, the causative agent of leaf spot which has negative effects on yield throughout the world, and *Curvularia trifolii*, which causes leaf blight and leaf spot on different type of feed crops [6]. Using healthy tobacco tissues as the source, we isolated and identified these two important parasitic species.

L. chartarum has a broad host range, usually confining its infections to *Triticum aestivum*, *Miscanthus giganteus*, *Withania somnifera*, *Bromus inermis Leyss*, and *Panicum virgatum cv. Alamo*, etc. [7-10]. It is noteworthy that the fruiting bodies of this fungus have been reported to cause facial eczema in some animals (i.e., sheep,

Preprints (www.preprints.org) | NOT PEER-REVIEWED | Posted: 8 July 2019 doi:10.20944/preprints201907.0119.v1

cattle, goats, and deer) due to the liver damage caused by a mycotoxin (sporidesmin) produced by the fungus [11-13]. Several studies have also described the presence of *L. chartarum* conidia in indoor air environments where asthma patients reside [14-15]. *C. trifolii*, as a high-temperature pathogen that is distributed worldwide, causes leaf spot on *Trifolium alexandrinum* (Berseem Clover) and leaf blight on Creeping Bentgrass [16-18]. Moreover, *C. trifolii* can produce different secondary metabolites during its culture. Among these, some show excellent anti-inflammatory and antitumor activity [19-22]. Given that there are great similarities in life style between *L. chartarum* and *C. trifolii*, they seem to be closely related and likely share similar genetic content and organization.

With the rapid development of new sequencing technologies, the mitogenomes of fungi have improved tremendously in recent years. The hundreds of available fungal mitogenomes in the public databases have provided an efficient resource for their classification, genetics, and analysis of their phylogenetic relationships. However, there are just several sequences published from the Pleosporales even in the class Dothideomycetes to which they belong [23-25]. Herein, we sequenced the complete mitochondrial genomes of *L. chartarum* and *C. trifolii*. Furthermore, we analysed and characterized the evolution and structural organization of *L. chartarum* and *C. trifolii* and compared these with other species in Pleosporales. The current results allow for an understanding of the gene content and evolutionary history of species in Pleosporales.

2. Materials and methods

Preprints (www.preprints.org) | NOT PEER-REVIEWED | Posted: 8 July 2019 doi:10.20944/preprints201907.0119.v1

2.1 Materials, isolation, and culture

The endophytic fungus *C. trifolii* was first isolated from the healthy leaves of *Nicotiana tabacum*, which was collected from Enshi, Hubei, P. R. China, in July 2016. The fungal strain *L. chartarum* was isolated from the fresh stems of *Nicotiana tabacum*, which was also collected from Enshi, Hubei. The fungi were identified by analysis of their internal transcribed spacer (ITS), V1, and V4 regions of rDNA, as described in our previous report [26], as well as by their morphologies. Both strains are currently deposited at the Tobacco Research Institute of Chinese Academy of Agricultural Sciences. In addition, a phylogenetic analysis of *C. trifolii* and *L. chartarum* based on the ITS1 region was performed using MEGA 6.0 [27].

2.2 DNA extraction

After isolation and purification, the hyphae of *C. trifolii* and *L. chartarum* were scraped from the surface of the agar, after which they were ground to a fine powder in the presence of liquid nitrogen. Genomic DNA was then extracted using a fungal DNA extraction kit (Omega Bio-tek, Norcross, GA, USA), following the manufacturer's instructions. Electrophoresis on 1% agarose gels was used to assess the integrity of DNA samples. The purity and concentration of these two samples were determined using a Nanodrop microspectrophotometer (ND-2000, Thermo Fisher Scientific, Waltham, MA, USA) and a Qubit 2.0. fluorometer (Life Technologies, Carlsbad, CA, USA), respectively. Genomic DNA was stored at -20°C prior to library construction.

2.3. Sequence assembly, annotation, and analysis

Preprints (www.preprints.org) | NOT PEER-REVIEWED | Posted: 8 July 2019 doi:10.20944/preprints201907.0119.v1

About 2 μg of genomic DNA from each strain was first fragmented into 500 bp fragments, followed by construction of an Illumina genome sequencing libraries using the NEBNext Ultra II DNA Library Prep Kits (NEB, Beijing, China) according to the manufacturer's instructions. These libraries were then sequenced on an Illumina HiSeq 2500 Platform (Illumina, San Diego, CA, USA). Briefly, raw sequence reads were first quality trimmed and adapter sequences were removed using FastQC software (version 0.11.5) [28]. Subsequently, the SPAdes 3.9.0 software package and MITObim V1.9 were used for the *de novo* assembly of the mitogenomes and the filling of contig gaps [29,30]. The complete mitogenomes of *C.trifolii* and *L.chartarum* have been deposited to GenBank (accession number of KY792993 and KY986975, respectively).

To annotate these two complete mitogenomes, their protein-coding genes (PCGs) were identified and annotated using NCBI Open Reading Frame Finder (http://www.ncbi.nlm.nih.gov/gorf/gorf.html), and further confirmed with BLASTP searches against the mitogenomes of two closely related species (*Bipolaris cookei*: MF784482.1 and *Pithomyces chartarum*: KY792993.1). Following this, tRNAs were identified using tRNAscan-SE 1.21 Search Server (http://lowelab.ucsc.edu/tRNAscan-SE/) with default settings [31]. rRNA genes were also identified using multi-sequence alignment with the GenBank sequences of *B. cookie* and *P. chartarum* mitogenomes using BLAST (http://blast.ncbi.nlm.nih.gov/Blast.cgi) searches. The base composition of these two mitogenomes were analysed with DNAStar Lasergene v7.1 (http://www.dnastar.com/). In addition, AT skews and GC skews were determined using (A%-T%)/(A%+T%) and (G%-C%)/(G%+C%) respectively to characterize

Preprints (www.preprints.org) | NOT PEER-REVIEWED | Posted: 8 July 2019 doi:10.20944/preprints201907.0119.v1

strand asymmetries in the mitogenomes. CodonW was used to analyse codon usage frequency for amino acids in these two genomes [32]. The graphical maps of these two mitogenomes were constructed using OGDRAW (http://ogdraw.mpimp-golm.mpg.de/cgi-bin/ogdraw.pl) [33].

2.4 Phylogenetic analysis

To determine the phylogenetic relationships of *C. trifolii* and *L. chartarum*, current available complete, or near-complete, mitochondrial genomes were used for phylogenetic analyses. The class Dothideomycetes includes the orders Botryosphaeriales, Pleosporales, and Capnodiales. Therefore, one species, *Mycosphaerella graminicola* which belongs to Capnodiales, was selected as an outgroup when the phylogenetic tree was constructed. Construction of the phylogenetic tree was performed using a combined dataset consisting of 12 common protein coding genes (*atp6*, *cob*, *cox1*, *cox2*, *cox3*, *nad1*, *nad2*, *nad3*, *nad4*, *nad4L*, *nad5*, and *nad6*) that are encoded in *C. trifolii* and *L. chartarum* and other related mitochondrial genomes. These genes were initially aligned with MAFFT using default settings and then concatenated head-to-tail to form the final datasets [34]. The nucleotide substitution models of the final datasets were selected using jModelTest [35]. Finally, the phylogenetic tree was constructed using RAxML version 8.1.12 [36] and MrBayes [37]. For each node of the maximum likelihood (ML) tree, the bootstrap support was calculated using 1000 replicates. For the Bayesian tree, the initial 10% of trees were discarded as burn-in, and four simultaneous chains were run for 10,000,000 generations.

Preprints (www.preprints.org) | NOT PEER-REVIEWED | Posted: 8 July 2019 doi:10.20944/preprints201907.0119.v1

3. Results and Discussion

3.1 Fungal isolation and identification

The strains studied here were identified as *C. trifolii* and *L. chartarum* on the basis of their morphologies and sequences of their ITS regions (Figure S1). The BLAST search results for ITS1 and ITS4 showed that their sequences were most similar (99.64% and 99.82%) to the same sequences obtained from the *C.trifolii* isolate FUNBIO-2 (GenBank Accession No. KC415610.1) and the *C .trifolii* strain AL9m5_2 18S (GenBank Accession No. KJ188716.1), respectively. Both the ITS1 and ITS4 sequences showed high identity to *L. chartarum*, especially for ITS4, which reached up to 100% identify with the *L. chartarum* strain KNU14-16 (GenBank Accession No. KP055597.1). Our results from the phylogenetic tree analysis supported these alignment results. The phylogenomic investigation of ITS1 sequence demonstrated that strain was *C. trifolii*. In our analysis, the phylogenetic relationships based on ITS1 also showed that the *L. chartarum* strain had high bootstrap value of 99%.

3.2 General features of the newly sequenced mitochondrial genomes

The complete sequence of the *L. chartarum* mitochondrial genome was mapped to be a 68,926 bp long circular molecule with an average GC content of 28.60%. The *C. trifolii* mitogenome was also a typical circular DNA molecule 59,100 bp in length with an average GC content of 29.31% (Figure 1). In the *L. chartarum* mitogenome, we

Preprints (www.preprints.org) | NOT PEER-REVIEWED | Posted: 8 July 2019 doi:10.20944/preprints201907.0119.v1

identified 36 protein coding genes, 26 tRNA genes, and 2 rRNA genes (rrnL and rrnS), which were located on both strands. Among the protein coding genes, 11 of these having identified functions while the remaining genes are ORFs. In total, we found 12 introns which were located in *cox1&2* (7), *nad5* (2), *cob* (2), and *cox3* (1) (Table 1). In the *C. trifolii* mitogenome, there were 26 protein coding genes, 30 tRNA genes, and 2 rRNA genes (rrnL and rrnS) (Table 2). We also found 22 introns which were distributed in the *atp6* (2), *nad1* (4), *cob* (4), *cox2* (4), and *cox1* (4) genes.

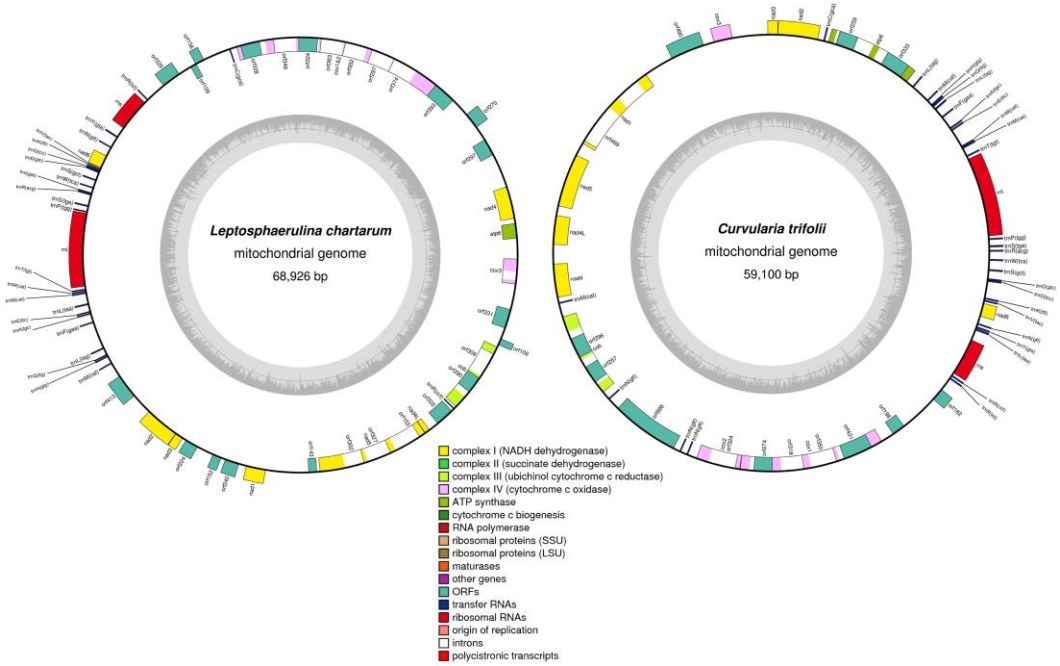

Figure 1. Circular maps of the complete mitochondrial genomes from *Leptosphaerulina chartarum* and *Curvularia trifolii*

Table 1. Organization of the mitochondrial genome of *Leptosphaerulina chartarum*

Gene	R/F	position	Length	Codon

Preprints (www.preprints.org) | NOT PEER-REVIEWED | Posted: 8 July 2019 doi:10.20944/preprints201907.0119.v1

		From	To	nt	aa	Start	Stop	Intergenic nucleotides
atp6	R	836	1606	771	257	AAT	GTA	194
nad4	R	1849	3504	1656	552	AAT	GTA	242
orf297	R	5240	6133	894	298	GAT	GTA	1735
orf270	F	6871	7683	813	271	ATG	TAG	737
orf393	R	8667	9848	1182	394	AAT	GTA	983
cox1&2	R	9752	20506	1266	422	GAT	GTA	-97
orf374	R	11196	12320	1125	375	AAT	AAC	-9311
orf297	R	12640	13533	894	298	GAT	ACA	319
orf352	R	13880	14938	1059	353	GAT	AGT	346
orf363	R	15081	16172	1092	364	AAT	AAC	142
orf324	R	16344	17318	975	325	AAT	GCA	171
orf349	R	17553	18602	1050	350	AAT	AAA	234
orf328	R	19307	20293	987	329	AAT	AAG	704
trnC(gca)	R	20817	20887	71		TCT	GGG	523
orf156	F	22265	22735	471	157	ATG	TAG	1377
orf109	R	22708	23037	330	110	GAT	GTA	-28
orf329	F	23702	24691	990	330	ATG	TAG	664
trnR(tct)	F	25731	25801	71		TTC	AAT	1039
rns	F	25961	27638	1678	559	TTA	ATT	159
trnY(gta)	F	28148	28232	85		AGG	CTA	509
trnN(gtt)	F	28767	28837	71		GCC	GCT	534
nad6	F	29284	29958	675	225	ATG	TAA	446
trnV(tac)	F	29909	29981	73		AAG	TTA	-50
trnK(ttt)	F	30009	30080	72		GAG	TTG	27

Preprints (www.preprints.org) | NOT PEER-REVIEWED | Posted: 8 July 2019 doi:10.20944/preprints201907.0119.v1

trnG(tcc)	F	30090	30160	71		ACG	GTA	9
trnD(gtc)	F	30163	30235	73		GGG	TCG	2
trnS(gct)	F	30586	30665	80		GGA	CCG	350
trnW(tca)	F	30995	31066	72		AAG	TTG	329
trnI(gat)	F	31284	31355	72		GGT	TCA	217
trnR(acg)	F	31359	31430	72		AGT	CTT	3
trnS(tga)	F	31940	32024	85		AGA	CTG	509
trnP(tgg)	F	32240	32312	73		CGG	CGA	215
rnl	F	32353	36047	3695	1231	TAT	CTG	40
trnT(tgt)	F	36169	36239	71		GCT	GCT	121
trnM(cat)	F	36261	36331	71		TGC	CAT	21
trnM(cat)	F	36349	36421	73		AAG	TTA	17
trnL(taa)	F	36916	36998	83		ATC	ATA	494
trnE(ttc)	F	37317	37389	73		GGC	CTT	318
trnA(tgc)	F	37414	37485	72		GGG	CCA	24
trnF(gaa)	F	37868	37940	73		GCC	GCA	382
trnL(tag)	F	39268	39350	83		ATG	ATA	1327
trnQ(ttg)	F	39645	39716	72		TAT	TAG	294
trnH(gtg)	F	39731	39804	74		GGT	TCC	14
trnM(cat)	F	40128	40198	71		GCC	GCT	323
orf413	F	40936	42177	1242	414	ATG	TAA	737
nad2	F	43265	45013	1749	583	ATG	TAA	1087
nad3	F	45014	45436	423	141	ATG	TAG	0
orf224	F	45621	46295	675	225	ATG	TAA	184
orf152	F	47163	47621	459	153	ATG	TAG	867
orf240	F	47835	48557	723	241	ATG	TAA	213

Preprints (www.preprints.org) | NOT PEER-REVIEWED | Posted: 8 July 2019 doi:10.20944/preprints201907.0119.v1

nad1	F	48948	49940	993	331	ATG	TAA	390
orf143	R	52108	52539	432	144	GAT	GTA	2167
nad5	R	52687	58415	1272	1909	GAT	GTA	147
orf302	R	54083	54991	909	303	AAT	GTT	-4333
orf327	R	55431	56414	984	328	AAT	AAA	439
orf103	R	57780	58091	312	104	AAT	GGC	1365
nad4L	R	58415	58684	270	90	AAT	GTA	323
orf322	R	59200	60168	969	323	AAT	GTA	515
trnR(cct)	R	60278	60348	71		GGA	CTC	109
cob	R	60443	64134	677	1230	AAT	GTA	94
orf290	R	61449	62321	873	291	GAT	ACA	-2686
orf309	R	62812	63741	930	310	AAT	GTT	490
orf109	F	64266	64595	330	110	ATG	TAA	524
rnpB	R	64844	65014	171	57	TAT	GAC	248
orf331	R	65157	66152	996	332	GAT	GTA	142
cox3	R	67443	68731	179	429	AAT	GTA	1290

Table 2. Organization of the mitochondrial genome of *Curvularia trifolii*

Gene	R/F	position		Length		Codon		Intergenic nucleotides
		From	To	nt	aa	Start	Stop	
trnR(acg)	F	59	130	72		AGT	CTT	117
trnS(tga)	F	248	332	85		AGA	CTG	230
trnP(tgg)	F	563	635	73		CAG	TGA	99
rnl	F	735	4181	3447	1149	TAT	TTA	99

Preprints (www.preprints.org) | NOT PEER-REVIEWED | Posted: 8 July 2019 doi:10.20944/preprints201907.0119.v1

trnT(tgt)	F	4281	4351	71		GCC	GCT	323
trnM(cat)	F	4675	4745	71		TGC	CAT	5
trnM(cat)	F	4751	4823	73		AAG	TTA	752
trnE(ttc)	F	5576	5648	73		GGC	CTT	32
trnA(tgc)	F	5681	5752	72		GGG	CCA	516
trnF(gaa)	F	6269	6341	73		GCC	GCA	378
trnL(tag)	F	6720	6802	83		ATG	ATA	77
trnQ(ttg)	F	6880	6951	72		TAT	TAA	4
trnH(gtg)	F	6956	7029	74		GGT	TCC	196
trnM(cat)	F	7226	7297	72		GCC	GCT	788
trnL(tag)	F	8086	8158	73		CGG	TGA	311
atp6	F	8470	12281	341	113	ATG	TAG	-3470
orf333	F	8812	9813	1002	334	AAA	TAA	1349
orf259	F	11163	11942	780	260	ATG	TAG	496
trnC(gca)	F	12439	12510	72		GGG	CCT	246
nad2	F	12757	14487	1731	577	ATG	TAA	0
nad3	F	14488	14925	438	146	ATG	TAA	1536
cox3	F	16462	17271	810	270	ATG	TAA	463
orf490	F	17735	19207	1473	491	ATG	TAA	1323
nad1	R	20531	24611	480	160	AAT	GTA	-1554
orf469	R	23058	24467	1410	470	AAT	TGT	699
nad5	R	25167	27509	2343	781	AAT	GTA	402
nad4L	R	27912	29189	1278	426	GAT	GTA	826
nad4	R	30016	31485	1470	490	AAT	GTT	204
trnM(cat)	R	31690	31760	71		TAA	CTT	576
cob	R	32337	36050	668	222	GAT	GTA	-2702

Preprints (www.preprints.org) | NOT PEER-REVIEWED | Posted: 8 July 2019 doi:10.20944/preprints201907.0119.v1

orf296	R	33349	34239	891	297	AAT	AAA	486
orf257	R	34726	35499	774	258	GAT	GTA	895
trnN(gtt)	R	36395	36465	71		TCG	CCG	508
orf996	R	36974	39964	2991	997	AAT	GTA	270
trnN(gtt)	R	40235	40305	71		TCG	CCG	260
trnN(gtt)	R	40566	40636	71		TCG	CCG	395
cox2	R	41032	42968	522	174	GAT	TAG	-1170
orf324	R	41799	42773	975	325	AAT	TTA	195
cox1	R	42969	49330	391	130	TGT	GTA	-5770
orf274	R	43561	44385	825	275	AAT	GGA	406
orf318	R	44792	45748	957	319	AAT	AAA	405
orf350	R	46154	47206	1053	351	AAT	AAA	333
orf431	R	47540	49935	1296	432	AAT	ATG	-27
orf198	R	49909	50505	597	199	AAT	GTA	1701
orf182	F	52207	52755	549	183	ATG	TAG	570
trnR(tct)	F	53326	53396	71		TTC	AAT	64
trnR(cct)	F	53461	53531	71		TTC	AAA	95
rns	F	53627	55255	1629	543	TTT	ATT	445
trnL(taa)	F	55701	55783	83		ATC	ATA	16
trnY(gta)	F	55800	55884	85		AGG	CTA	81
trnN(gtt)	F	55966	56036	71		GTT	GCT	304
nad6	F	56341	56916	576	192	ATG	TAA	81
trnV(tac)	F	56998	57070	73		AAG	TTA	32
trnK(ttt)	F	57103	57174	72		GAG	TTA	690
trnG(tcc)	F	57865	57936	72		GCG	GTA	2
trnD(gtc)	F	57939	58010	72		GGG	TCG	317

Preprints (www.preprints.org) | NOT PEER-REVIEWED | Posted: 8 July 2019 doi:10.20944/preprints201907.0119.v1

trnS(gct)	F	58328	58407	80		GGA	CCG	364
trnW(tca)	F	58772	58843	72		AAG	TTG	-58844

Both the GC content and the gene content of the complete mitogenomes of *L. chartarum* and *C. trifolii* are comparable to previously reported mitogenomes of species in Pleosporales [25]. The genome sizes of these mitogenomes are larger than the closely related species *Shiraia bambusicola* (39,030 bp), *Phaeosphaeria nodorunm* (49,761bp) and *Bipolaris maydis* (37,250 bp), while being much smaller that the mitogenomes of *Leptosphaeria maculans* (154,863bp) and *Pyrenophora tritici-repentis* (15,7011bp). At least one group I and few group II introns are found in most fungal mitogenomes. For example, there are 39 introns in the *Pezizomycotina subphylum* mitogenome and 2 in the *Fusarium oxysporum* mitogenome [38]. However, in a previous study we did not find any introns in the *Mycosphaerella graminicola* mitogenome [23]. It is noteworthy that the differences in the number of ORFs and the presence of introns may be attributed to the various sizes of the fungi mitogenomes, which is consistent with previous studies [39-41].

3.3 Gene content and structural comparison

In the *L. chartarum* and *C. trifolii* mitochondrial genomes, the whole genomes contained 36 and 26 protein coding genes, respectively. The entire length of the protein coding genes of *L. chartarum* occupied 38.62% of the whole genome, while that of *C. trifolii* occupied 84.02%. The overall G+C content of the protein coding genes was 29.78% in the *L. chartarum* mitogenome, ranging from 21.21% (ORF109) to 43.17% (ORF270)

Preprints (www.preprints.org) | NOT PEER-REVIEWED | Posted: 8 July 2019 doi:10.20944/preprints201907.0119.v1

(Table 3). In the *C. trifolii* mitogenome, the G+C content of the protein coding genes was 28.12%, ranging from 22.92% (*nad6*) to 32.23% (*cox1*) (Table 4). The mitochondrial genome codon usage in *L. chartarum* and *C. trifolii* showed a significant bias towards A and T, as is found other fungal species [42, 43]. In the *L. chartarum* and *C. trifolii* mitochondrial genomes, Ile, Leu, Lys, and Phe are the most frequently encoded amino acids, and we found that UUU, AUU, AAU, and UAU are the most frequent codons in both of these genomes. Since these frequently used codons are exclusively comprised of A and T (U) (Figure 2), this contribute to the high A + T content seen in most fungal mitochondrial genomes such as in *Beauveria pseudobassiana* and *Madurella mycetomatis* [44,45]. This preferred codon usage is strongly reflected at the third position by the high A/T versus G/C frequencies (Table S1), which is consistent with the rich A+T content in the whole mitogenomes.

Table 3. AT-content, AT-skew and GC-skew for mitochondrial genes of *Leptosphaerulina chartarum*

Feature	A%	C%	G%	T%	(A+T)%	AT skew	GC skew
Whole genome	35.99	14.19	14.43	35.39	71.38	0.01	0.01
Protein-coding genes	35.33	14.65	15.14	34.89	70.22	0.01	0.02
cox1&2	36.73	16.43	16.19	30.65	67.38	0.09	-0.01
cox3	41.34	17.32	12.29	29.05	70.39	0.17	-0.17
cob	40.92	15.36	14.62	29.10	70.01	0.17	-0.02
nad1	28.50	12.99	15.21	43.30	71.80	-0.21	0.08
nad2	34.71	12.98	12.81	39.51	74.21	-0.06	-0.01
nad4	32.86	12.77	13.24	41.13	74.00	-0.11	0.02

Preprints (www.preprints.org) | NOT PEER-REVIEWED | Posted: 8 July 2019 doi:10.20944/preprints201907.0119.v1

nad4L	40.70	15.28	13.41	30.62	71.32	0.14	-0.07
nad5	40.57	15.71	10.00	33.71	74.29	0.09	-0.22
nad6	38.99	14.47	14.62	31.92	70.91	0.10	0.01
atp6	40.34	12.71	14.27	32.68	73.02	0.10	0.06
orf103	27.56	20.83	13.78	37.82	65.38	-0.16	-0.20
orf109	43.33	12.12	11.21	33.33	76.67	0.13	-0.04
orf109	36.06	8.48	12.73	42.73	78.79	-0.08	0.20
orf143	34.03	15.97	13.89	36.11	70.14	-0.03	-0.07
orf152	35.08	12.42	13.94	38.56	73.64	-0.05	0.06
orf156	44.16	13.16	11.25	31.42	75.58	0.17	-0.08
orf224	34.37	15.41	16.59	33.63	68.00	0.01	0.04
orf240	41.49	8.58	15.08	34.85	76.35	0.09	0.27
orf270	30.01	20.79	22.39	26.81	56.83	0.06	0.04
orf290	37.92	12.71	12.60	36.77	74.68	0.02	0.00
orf297	24.05	23.27	19.35	33.33	57.38	-0.16	-0.09
orf297	32.89	17.79	13.31	36.02	68.90	-0.05	-0.14
orf302	34.43	13.75	12.54	39.27	73.71	-0.07	-0.05
orf309	33.44	14.62	12.90	39.03	72.47	-0.08	-0.06
orf322	36.12	17.75	16.31	29.82	65.94	0.10	-0.04
orf324	31.79	15.08	12.41	40.72	72.51	-0.12	-0.10
orf327	33.54	16.06	12.60	37.80	71.34	-0.06	-0.12
orf328	32.22	15.50	12.46	39.82	72.04	-0.11	-0.11
orf329	40.30	9.49	15.66	34.55	74.85	0.08	0.24
orf331	37.55	12.95	14.06	35.44	72.99	0.03	0.04
orf349	33.52	14.95	13.05	38.48	72.00	-0.07	-0.07
orf352	32.58	17.85	16.81	32.77	65.34	0.00	-0.03

Preprints (www.preprints.org) | NOT PEER-REVIEWED | Posted: 8 July 2019 doi:10.20944/preprints201907.0119.v1

orf363	34.43	15.11	11.54	38.92	73.35	-0.06	-0.13
orf374	35.02	13.51	11.38	40.09	75.11	-0.07	-0.09
orf393	31.05	18.87	14.21	35.87	66.92	-0.07	-0.14
orf413	42.35	9.58	13.61	34.46	76.81	0.10	0.17
rnpB	28.65	14.62	14.04	42.69	71.35	-0.20	-0.02
tRNAs	41.53	24.88	33.51	48.61	90.14	-0.08	0.15
rns	33.08	15.49	22.11	29.32	62.40	0.06	0.18
rnl	35.53	13.75	20.73	29.99	65.52	0.08	0.20
NCR	37.63	12.44	12.95	36.98	74.61	0.01	0.02

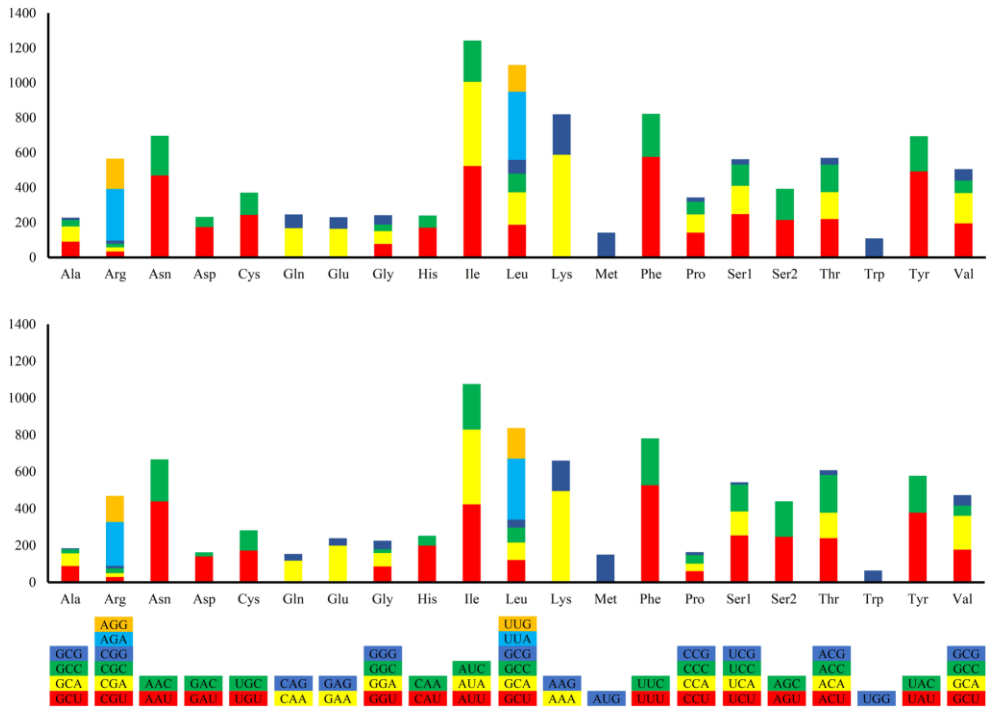

Figure 2 Mitochondrial genome codon usage in *Leptosphaerulina chartarum* and *Curvularia trifolii*

3.4 Transfer RNA and ribosomal RNA genes.

Preprints (www.preprints.org) | NOT PEER-REVIEWED | Posted: 8 July 2019 doi:10.20944/preprints201907.0119.v1

In total, 26 tRNAs were identified in the *L. chartarum* mitochondrial genome, which ranged from 70 bp (trnC(gca), trnG(tcc), trnM(cat)) to 84 bp (trnS(tga) and trnY(gta)) in length (Table 1). The results of the secondary structure analysis showed that all tRNAs harboured a typical cloverleaf structure, except for trnY-GTA, trnS-GCT, trnl-TAA, trnS-TGA, and trnL-TAG (Figure 3). In addition, we found some tRNAs, such as trnL-TAA and tRNAA-TAG, have the same anticodon. Moreover, we found that there are three copies of tRNAM which are located in different regions of the mitogenome. The *C. trifolii* mitochondrial genome contained 2,143 bp which encoded tRNA genes, with an A + T content of 90.14%. The individual tRNAs ranged in length from 71 bp (such as trnM(cat), trnM(cat) and trnN(gtt) etc.) to 85 bp (trnY(gta)). Twenty-nine tRNAs in the *C. trifolii* mitochondrial genome carried codons for 19 amino acids (Figure 4). Among these, we found some of them existed as multiple tRNAs (Table 2). For example, 4 tRNA genes were found to encode methionine. There were 2, 2, and 3 different tRNA genes for leucine (trnL-TAA and trnL-TAG), serine (trnS-GCT and trnS-TGA), and lysine (trnL-ACG, trnL-CCT and trnL-TCT), respectively in the *C. trifolii* mitochondrial genome. Two ribosomal RNA genes were found in the *L. chartarum* mitochondrial genome, namely rrnL and rrnS, which were 3,694 bp (with an A + T content of 65.52%) and 1,677 bp (with an A + T content of 62.40%) in length, respectively (Table 3). In the *C. trifolii* mitochondrial genome, the rrnL gene was 3,447 bp long, with an A + T content of 62.37% and the rrnS gene was1,629 bp long, with an A + T content of 62.40% (Table 4). All the tRNAs and

Preprints (www.preprints.org) | NOT PEER-REVIEWED | Posted: 8 July 2019 doi:10.20944/preprints201907.0119.v1

rRNAs from these two newly sequenced mitochondrial genomes are comparable to those in related species [46,47].

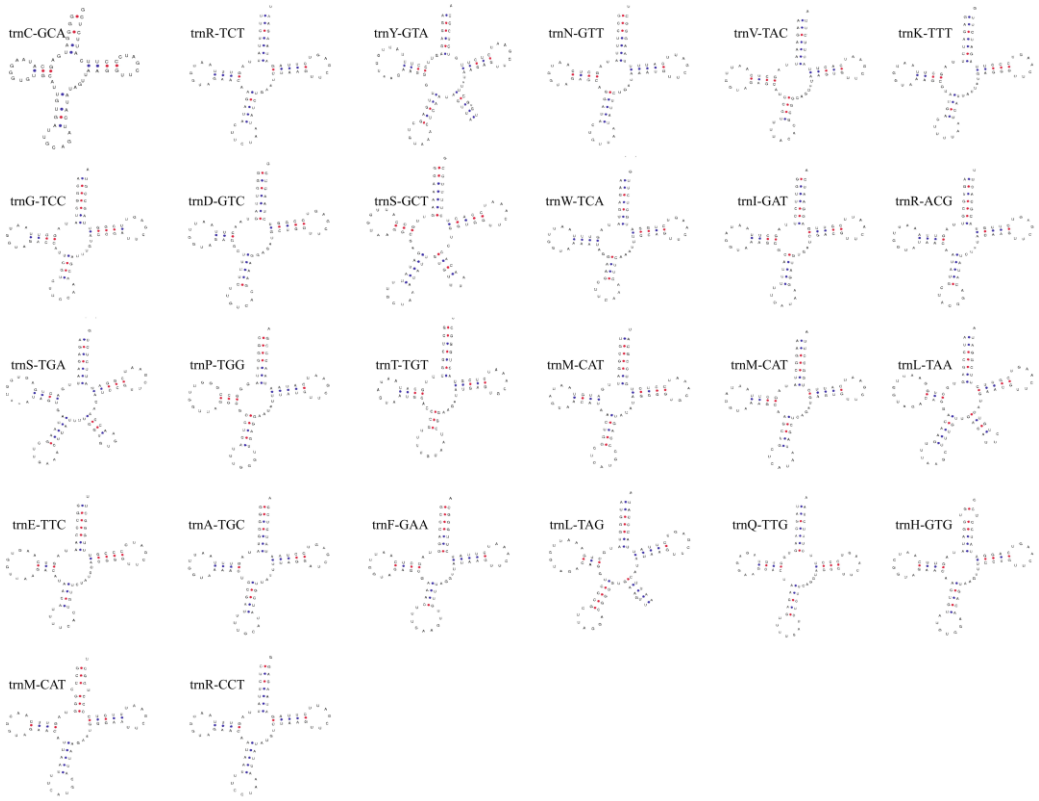

Figure 3. The predicted tRNA structures of *Leptosphaerulina chartarum*

Preprints (www.preprints.org) | NOT PEER-REVIEWED | Posted: 8 July 2019 doi:10.20944/preprints201907.0119.v1

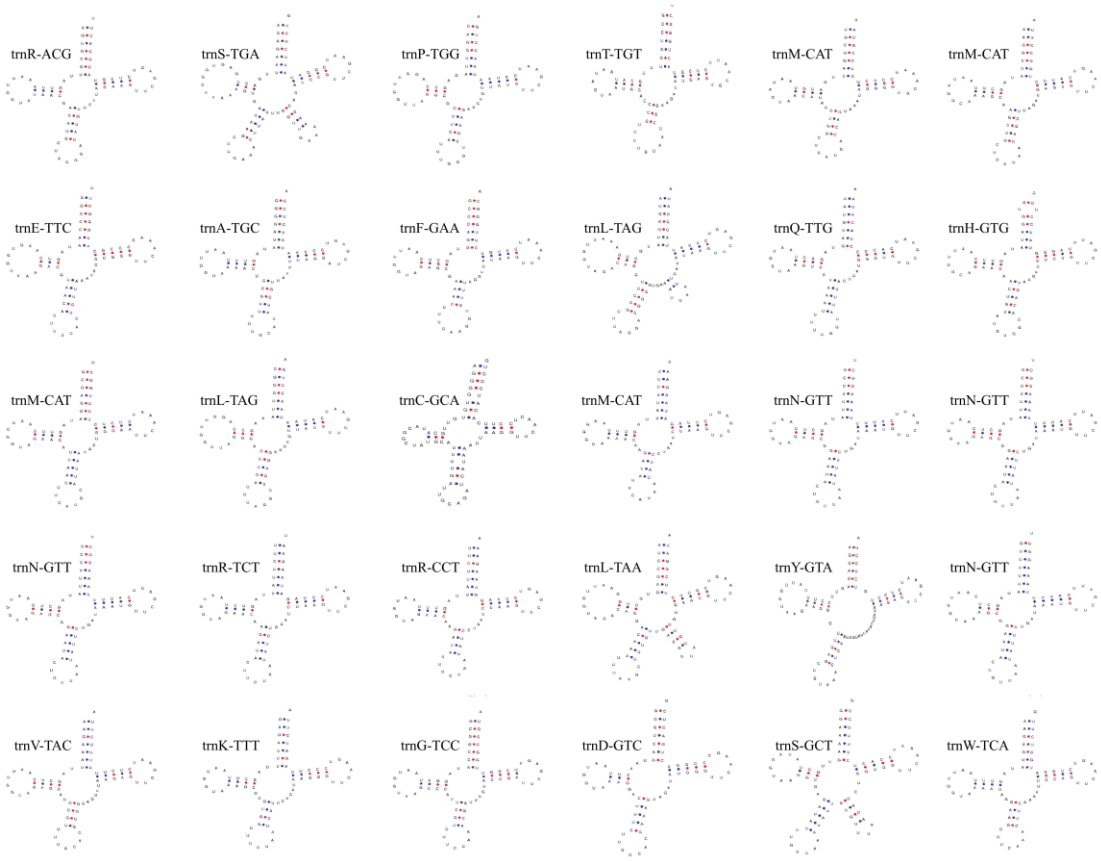

Figure 4. The predicted tRNA structures of *Curvularia trifolii*

Table 4. AT-content, AT-skew and GC-skew for mitochondrial genes of *Curvularia trifolii*

Feature	A%	C%	G%	T%	(A+T)%	AT skew	GC skew
Whole genome	35.15	14.55	14.75	35.54	70.69	-0.01	0.01
Protein-coding genes	35.86	14.59	13.53	36.02	71.88	0.00	-0.04
cox1	38.36	14.58	17.65	29.41	67.77	0.13	0.10
cox2	36.40	16.48	15.71	31.42	67.82	0.07	-0.02
cox3	29.26	15.43	16.79	38.52	67.78	-0.14	0.04
cob	39.37	15.27	16.02	29.34	68.71	0.15	0.02
nad1	41.88	15.00	13.13	30.00	71.88	0.17	-0.07
nad2	33.28	14.38	13.29	39.05	72.33	-0.08	-0.04

Preprints (www.preprints.org) | NOT PEER-REVIEWED | Posted: 8 July 2019 doi:10.20944/preprints201907.0119.v1

nad3	33.11	12.33	14.16	40.41	73.52	-0.10	0.07
nad4	42.31	13.54	13.67	30.48	72.79	0.16	0.01
nad4L	35.37	15.18	12.52	36.93	72.30	-0.02	-0.10
nad5	37.99	17.63	13.53	30.86	68.84	0.10	-0.13
nad6	34.72	9.72	13.19	42.36	77.08	-0.10	0.15
atp6	38.42	15.84	10.56	35.19	73.61	0.04	-0.20
orf182	35.34	12.02	15.48	37.16	72.50	-0.03	0.13
orf198	28.48	16.92	15.24	39.36	67.84	-0.16	-0.05
orf257	31.52	16.67	10.21	41.60	73.13	-0.14	-0.24
orf259	37.56	13.33	17.56	31.54	69.10	0.09	0.14
orf274	31.15	16.85	11.27	40.73	71.88	-0.13	-0.20
orf296	35.47	14.03	13.47	37.04	72.50	-0.02	-0.02
orf318	33.44	15.26	12.75	38.56	72.00	-0.07	-0.09
orf324	30.26	16.82	14.36	38.56	68.82	-0.12	-0.08
orf333	40.92	12.28	14.07	32.73	73.65	0.11	0.07
orf350	32.67	14.53	13.68	39.13	71.79	-0.09	-0.03
orf431	32.48	15.51	13.66	38.35	70.83	-0.08	-0.06
orf469	36.17	14.04	10.57	39.22	75.39	-0.04	-0.14
orf490	43.31	10.86	12.90	32.93	76.24	0.14	0.09
orf996	36.04	13.81	13.24	36.91	72.95	-0.01	-0.02
tRNAs	29.02	16.92	21.34	32.72	61.73	-0.06	0.12
rns	35.28	14.22	20.37	30.14	65.42	0.08	0.18
rnl	32.11	15.04	22.59	30.26	62.37	0.03	0.20
NCR	35.08	13.38	14.06	37.48	72.56	-0.03	0.02

Preprints (www.preprints.org) | NOT PEER-REVIEWED | Posted: 8 July 2019 doi:10.20944/preprints201907.0119.v1

3.5 Comparison of the mitogenome components

In order to understand the variation in mitogenome components between *L. chartarum* and *C. trifolii* and related species, a comparative analysis of the protein-coding gene was performed. Five representative species from Pleosporales, namely *L. chartarum*, *C. trifolii*, *Phaeosphaeria nodorum*, *S. bambusicola*, and *Didymella pinodes*, were used for the mitogenome component comparison. As shown in Figure 5, the order of the protein-coding genes showed that gene rearrangements had occurred among the different Pleosporales species. For the mitogenomes from *L. chartarum* and *C. trifolii*, there were three representative regions, including block 1 (*rns-nad6-rnl*), block 2 (*nad2-nad4*) and block 3 (*cox1* and *cox2*) (Figure 5). In block 1, the analysis showed that *rns-nad6-rnl* is a conserved region in all species. A comparison the genes in block 2 showed that *L. chartarum* and *C. trifolii* were more similar to each other than those in other species. The gene arrangement of *nad2-nad3* in block 2 showed a diverse range of patterns and different orientations. Moreover, some specific genes were found to cluster together, indicating a strong relationship. For example, the gene pair *nad5–nad4L* was present in all ten of the mitochondrial genomes analysed. In block 3, it is noteworthy that *cox1* and *cox2* showed a different pattern in *S. bambusicola* and that the *cox3* gene also showed little diversity in its gene order among these five species. The data showed that *rps3* only exists in *L.chartarum*, while it is absent from the other four species. A comparison of *L. chartarum* and *C. trifolii* mtDNAs indicated that these two related species had an identical mitochondrial gene order and gene orientation.

Preprints (www.preprints.org) | NOT PEER-REVIEWED | Posted: 8 July 2019 doi:10.20944/preprints201907.0119.v1

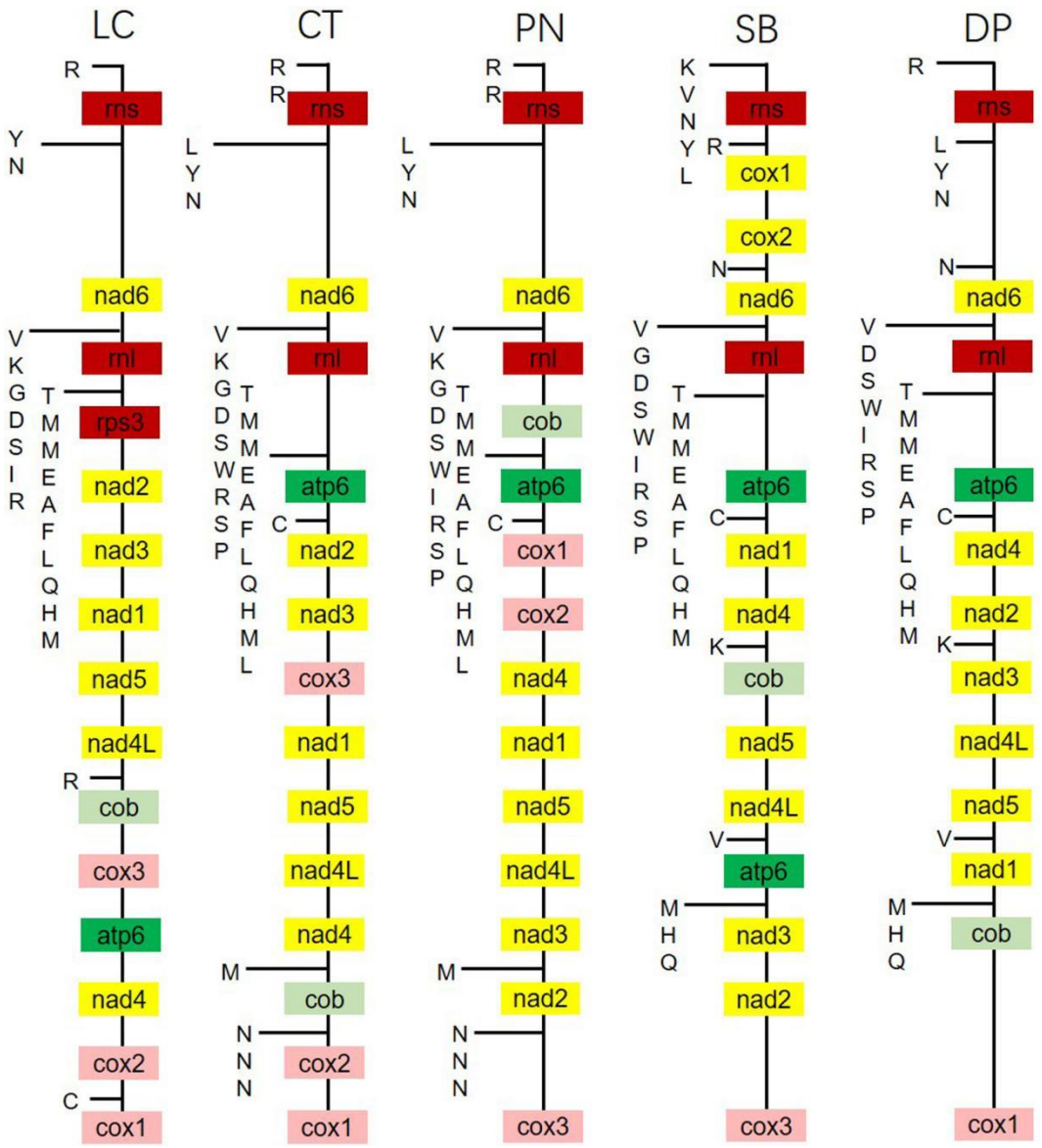

Figure 5 Mitochondrial gene orders in five species

3.6 Phylogenetic relationship

In order to gain additional evidence for the classification of Pleosporales species and to understand the evolutionary history of the mitochondrial genome, the complete concatenated amino acid sequences of the 12 standard mitochondrial genes (*atp6*, *cox1*, *cox2*, *cox3*, *nad1*, *nad2*, *nad3*, *nad4*, *nad4L*, *nad5*, *nad6*, and *cob*) were used for a phylogenetic construction by maximum parsimony (Figure 6). The model GTR + I

Preprints (www.preprints.org) | NOT PEER-REVIEWED | Posted: 8 July 2019 doi:10.20944/preprints201907.0119.v1

+ G was chosen for the combined sequences. Both ML and Bayesian analyses produced inconsistent topologies (Figure 6). *M. graminicola* was located in the basal position of the phylogenetic tree. In the Pleosporales group, *L. chartarum* and *C.trifolii* were found to be sister groups with high confidence (100% for bootstrap and 1 for BI). This clade clustered with the clade containing the other five species *P. tritici-repentis*, *P. nodorunm*, *L. maculans*, *D. pinodes*, and *B. maydis.* Among this clade, *L. maculans* was located in the medium position of these species and was therefore separated from (*P. tritici-repentis*, *P. nodorunm*) and (*D. pinodes* and *B. maydis*). It appears that *S. bambusicola* is at a greater genetic distance from other species in Pleosporales. The results from our study are therefore consistent with previous studies [25]. As mentioned above, there are just several mitogenomes have been published from the Pleosporales even in the class Dothideomycetes belongs to [23-25]. The complete mitogenomes of *L. chartarum* and *C. trifolii* will provide more effective information for us to understand the phylogenetic relationship of species among Pleosporales.

Preprints (www.preprints.org) | NOT PEER-REVIEWED | Posted: 8 July 2019 doi:10.20944/preprints201907.0119.v1

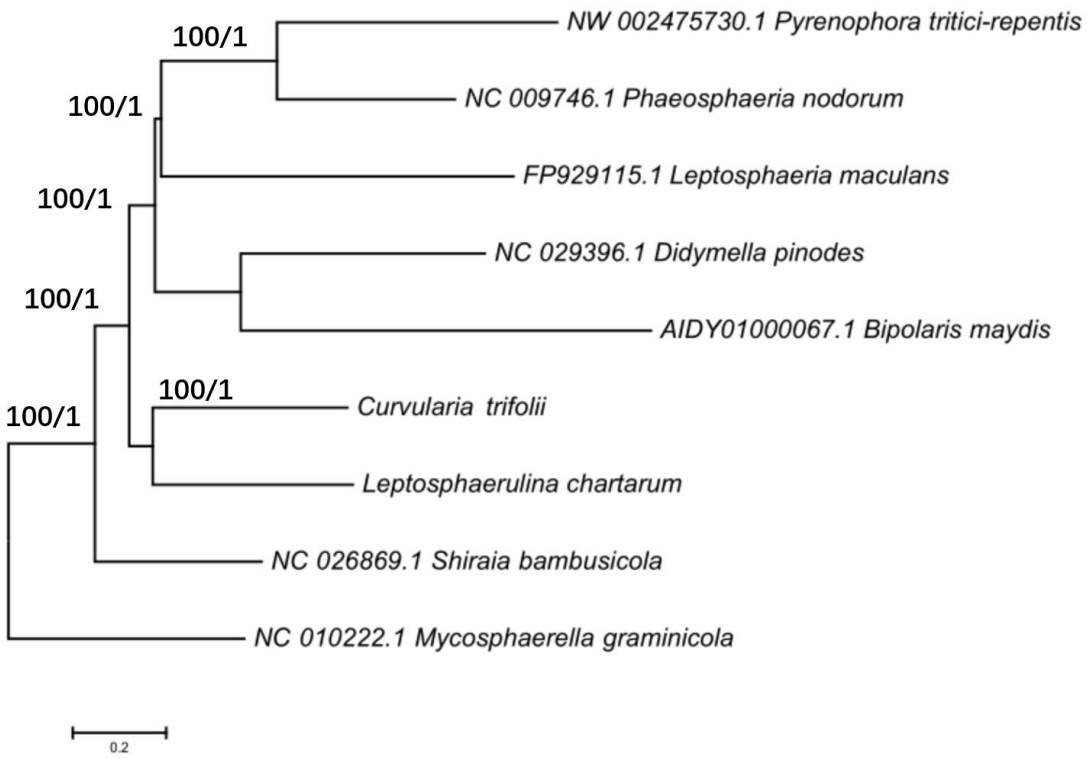

Figure 6 Phylogenetic trees constructed by the ML and BI methods based on 12 common protein coding genes. Species used in this study. *Leptosphaerulina chartarum* and *Curvularia trifolii* (in this study); *Shiraia bambusicola* (NC_026869.1); *Didymella pinodes* (NC_029396.1); *Bipolaris maydis* (AIDY01000067 and AIDY01000043)); *Leptosphaeria maculans* (FP929115); *Pyrenophora tritici-repentis* (NW002475730); *Phaeosphaeria nodorunm* (NC009746); *Mycosphaerella graminicola* (NC010222).

4. Conclusions

Fungal endophytes in tobacco are widely distributed in almost all tissues and play a very important role because they have a variety of different biological functions. Therefore, it is important to determine the species distribution and characteristics of endophytic fungi in tobacco. Using healthy tissues from tobacco as the source, we

Preprints (www.preprints.org) | NOT PEER-REVIEWED | Posted: 8 July 2019 doi:10.20944/preprints201907.0119.v1

isolated and identified two endophytic fungi namely *L. chartarum* and *C. trifolii* and obtained the sequences of their mitogenomes. We successfully annotated their protein-coding genes, compared their gene content and A+T content, and then constructed their phylogenetic relationship with other available species in Pleosporales. These data provide us with new insights to determining the species distribution and characteristics of endophytic fungi in tobacco.

Author Contributions: P. Z and Z.-F.Z. conceived and designed the project. X.-L.Y. and M.C. performed the experiments. G.-M.S., H.-B. Z and Y.-M.D. drafted and revised the manuscript. Q.L, L.X., J.-M.G, and Y.-M.D. analyzed and interpreted the data. All authors have read and approved the final manuscript.

Funding: This work was supported by the Natural Science Foundation of China (grant number 31700295)，the Science Foundation for Young Scholars of Institute of Tobacco Research of Chinese Academy of Agricultural Sciences (grant number 2016A02)，and the Agricultural Science and Technology Innovation Program (Grant No. ASTIP-TRIC05).

Conflicts of interest: The authors declare that the research was conducted in the absence of any commercial or financial relationships that could be construed as a potential conflict of interest.

Preprints (www.preprints.org) | NOT PEER-REVIEWED | Posted: 8 July 2019 doi:10.20944/preprints201907.0119.v1

References

1.Spurr H.W. ; R.E. Welty. Characterization of endophytic fungi in healthy leaves of nicotiana spp. *Phytopathology* **1975**, 65, 417–422.

2. Li X.; Li X.; Zhao K.;Wang R.; Zhang X. Diversity of the rhizosphere soil culture-dependent fungi of mature tobacco. *Am. J. Microbiol.* **2011**, 2, 9–14.

3. Norse D. Fungi isolated from surface-sterilized toabcco leaves. *Transact. Brit. Mycol. Soc.* **1972**, 58, 515–518.

4. Wanasinghe D.N.; Jewon R.; Jones E.B.G.; Boonmee S. Novel palmicolous taxa within Pleosporales: multigene phylogeny and taxonomic circumscription. *Mycol. Prog.* **2018**, 17, 571–590.

5. Yuan X.L.; Cao M.; Liu X.M.; Du Y.M.; Shen G.M.; Zhang Z.F.; Li J.H.; Zhang P. Composition and genetic diversity of the *Nicotiana tabacum* microbiome in different topographic areas and growth periods. *Int. J. Mol. Sci.* **2018**, 19, 3421

6. Kodsueb R.; Dhanasekaran V.; Aptroot A.; Lumyong S.; McKenzie E.H.; Hyde K.D.; Jeewon R. The family Pleosporaceae: intergeneric relationships and phylogenetic perspectives based on sequence analyses of partial 28S rDNA. *Mycologia* **2006**, 98, 571–583.

7. Eken C.; Jochum C.C.; Yuen G.Y. First report of leaf spot of smooth bromegrass caused by Pithomyces chartarum in Nebraska. *Plant Dis.* **2006**, 90, 108.

Preprints (www.preprints.org) | NOT PEER-REVIEWED | Posted: 8 July 2019 doi:10.20944/preprints201907.0119.v1

8. Tóth B.; Cso˝sz M.; Dijksterhuis J.; Frisvad J.C.; Varga J.Pithomyces chartarum as a pathogen of wheat. *J. Plant Pathol.* **2007**, 89, 405–408.

9. Verma R.K.; Sharma A.K.; Gupta B.D. Surface plasmon resonance based tapered fiber optic sensor with different taper profiles. *Opt. Commun.* **2008**, 281, 1486–1491.

10.. Ahonsi M.; Ames K.A.; Gray M.E.; Bradley C. Biomass reducing potential and prospective fungicide control of a new leaf blight of Miscanthus× giganteus caused by Leptosphaerulina chartarum. *Bioenergy Res.* **2013**, 6, 737–745.

11. Van Wuijckhuise L.; Snoep J.; Cremers G.; Duvivier A. Pithomycotoxicosis of facial eczema bij het rund voor de eerste maal aangetoond in Nederland. *Tijdschr. Diergeneesk.* **2006**, 131, 858–861.

12. Ozmen O.; Sahinduran S.; Haligur M.; Albay M.K. Clinicopathological studies on facial eczema outbreak in sheep in Southwest Turkey. *Trop. Anim. Health Prod.* **2008**, 40, 545–551.

13. Di Menna M.E.; Smith BL.; Miles C.O. A history of facial eczema (pithomycotoxicosis) research. *New Zeal. J. Ag. Res.* **2009**, 52, 345–376.

14. Jones R.; Recer G.M.; Hwang S.A.; Lin S. Association between indoor mold and asthma among children in Buffalo. *New York, Indoor Air* **2011**, 21, 156–164.

15. Meng J.; Barnes C.S.; Rosenwasser L.J. Children's Mercy Center for Environmental Health, Identity of the fungal species present in the homes of asthmatic children. *Clin. Exp. Allergy* **2012**, 42, 1448–1458.

Preprints (www.preprints.org) | NOT PEER-REVIEWED | Posted: 8 July 2019 doi:10.20944/preprints201907.0119.v1

16. Falloon R.E. *Cavalleria trifolii* as a high-temperature turfgrass pathogen. *New Zeal. J. Ag. Res.* **1976**, 19, 243-248.

17. Khadka R.B. First report of *Curvularia trifolii* causing leaf spot on *Trifolium alexandrinum* (Berseem Clover) in Nepal. *Plant Dis.* **2016**, 100, 1246.

18. SungC.H.; Koo J.H.; Kim J.H.; Yoon J.H. First report of *Curvularia* leaf blight caused by *Curvularia trifolii* on Creeping bentgrass in Korea. *Weed Turfgrass Sci.* **2016**, 5, 101–104.

19. Couttolenc A.; Espinoza C.; Fernández J.J.; Norte M.; Plata G.B.; Padrón J.M.; Shnyreva A.; Trigos A. Antiproliferative effect of extract from endophytic fungus *Curvularia trifolii* isolated from the “Veracruz Reef System” in Mexico". *Pharm. Biol.* **2016**, 54, 1392–1397.

20. Devpura S.N.; Samanthi U.; Paranagama P.A. In vitro antibacterial activities of secondary metabolites found in the endolichenic fungus, Curvularia trifolii inhabiting the lichen, Usnea sp. from Hakgala montane forest in Sri Lanka. *Proceedings of the 70th annual sessions of Sri Lanka Association for the Advancement of Science* **2014**.

21. Samanthi U.; Wickramarachchi S.; Wijeratne K.; Paranagama P. Two new bioactive polyketides from *Curvularia trifolii*, an endolichenic fungus isolated from Usnea sp., in Sri Lanka. *J. Natl. Sci. Found.* **2015**, 43, 217–224.

22. Espinoza C.; Couttolenc A.; Fernández J.J.; Norte M.; Plata G. B.; Padrón J.M.; Shnyreva A.,; Trigos Á. Brefeldin-A: an antiproliferative metabolite of the fungus

Preprints (www.preprints.org) | NOT PEER-REVIEWED | Posted: 8 July 2019 doi:10.20944/preprints201907.0119.v1

Curvularia trifolii collected from the Veracruz Coral Reef System, Mexico. *J. Mex. Chem. Soc.* **2016**, 60, 279–282.

23. Torriani S.F.; Goodwin S.B.; Kema G.H.; Pangilinan J.L.; McDonald B.A. Intraspecific comparison and annotation of two complete mitochondrial genome sequences from the plant pathogenic fungus *Mycosphaerella graminicola*. *Fungal Genet. Biol.* **2008**, 45, 628–637.

24. Hane J.K.; Lowe R.G.; Solomon P.S.; Tan K.C.; Schoch C.L.; Spatafora J.W.; Crous P.W.; Kodira C.; Birren B.W.; Galagan J.E.; Torriani S.F.; McDonald B.A.; Oliver R.P. Dothideomycete–plant interactions illuminated by genome sequencing and EST analysis of the wheat pathogen Stagonospora nodorum. *Plant Cell* **2007**, 19, 3347–3368.

25. Shen X.Y.; Li T.; Chen S.; Fan L.; Gao J.; Hou C.L. Characterization and phylogenetic analysis of the mitochondrial genome of Shiraia bambusicola reveals special features in the order of Pleosporales. *PloS one* **2015**, 10, e0116466.

26. Zhang P.; Mándi A.; Li X.M.; Du F.Y.; Wang J.N.; Li X.; Kurtán T.; Wang B.G. Varioxepine A a 3 H-oxepine-containing alkaloid with a new oxa-cage from the marine algal-derived endophytic fungus *Paecilomyces variotii*. *Org. Lett.* **2014**, 16, 4834–4837.

27. Tamura K., Stecher G., Peterson D., Filipski A., Kumar S. MEGA6: molecular evolutionary genetics analysis version 6.0. *Mol. Biol. Evol.* **2013**, 30, 2725–2729.

Preprints (www.preprints.org) | NOT PEER-REVIEWED | Posted: 8 July 2019 doi:10.20944/preprints201907.0119.v1

28. Andrews S. 2010. FastQC: a quality control tool for high throughput sequence data. Available online at: http://www.bioinformatics.babraham.ac.uk/projects/fastqc **2010**.

29. Bankevich A.; Nurk S.; Antipov D.; Gurevich A.A.; Dvorkin M.; Kulikov A.S.; LesinV.M.; Nikolenko S.I.; Pham S.; Prjibelski A.D.; PyshkinA.V.; Sirotkin A.V.; Vyahhi N.;. Tesler G; Alekseyev M.A.; Pevzner P.A. SPAdes: a new genome assembly algorithm and its applications to single-cell sequencing. *J. Comput. Biol.* **2012**, 19, 455–477.

30. Hahn C.; Bachmann L.; Chevreux B. Reconstructing mitochondrial genomes directly from genomic next-generation sequencing reads–a baiting and iterative mapping approach. *Nucleic Acids Res.* **2013**, 41, e129.

31. Lowe T.M.; Chan P.P tRNAscan-SE On-line: Search and Contextual Analysis of Transfer RNA Genes. *Nucl. Acids Res.* **2016**, 44, W54–57.

32. Peden J. CodonW version 1.4. 2, **2005**. Available at http://sourcforge.net/projects/codonw/

33. Lohse M.; Drechsel O.; Bock R. Organellar Genome DRAW (OGDRAW): a tool for the easy generation of high-quality custom graphical maps of plastid and mitochondrial genomes. *Curr. Genet.* **2007**, 52, 267–274

34. Katoh K.; Standley D.M. MAFFT multiple sequence alignment software version 7: improvements in performance and usability. *Mol. Biol. Evol.* **2013**, 30, 772–780.

Preprints (www.preprints.org) | NOT PEER-REVIEWED | Posted: 8 July 2019 doi:10.20944/preprints201907.0119.v1

35. Darriba D.; Taboada G.L.; Doallo R.; Posada D. jModelTest 2: more models, new heuristics and parallel computing. *Nat Methods* **2012**, 9, 772.

36. Stamatakis A. RAxML version 8: a tool for phylogenetic analysis and post-analysis of large phylogenies. *Bioinformatics* **2014**, 30, 1312–1313.

37. Huelsenbeck J.P.; Ronquist F. MRBAYES: Bayesian inference of phylogenetic trees. *Bioinformatics* **2001**, 17, 754-755.

38. Pantou M.P.; Kouvelis V.N.; Typas M.A. The complete mitochondrial genome of Fusarium oxysporum: insights into fungal mitochondrial evolution. *Gene* **2008**, 419, 7-–5.

39. Friedrich A.; Jung P.P.; Hou J.; Neuveglise C.; Schacherer J. Comparative mitochondrial genomics within and among yeast species of the Lachancea genus. *PLoS One* **2012**, 7, e47834.

40. Zhang Y.J.; Zhang S.; Zhang G.Z.; Liu X.Z.; Wang C.S.; Xu J.P. Comparison of mitochondrial genomes provides insights into intron dynamics and evolution in the caterpillar fungus *Cordyceps militaris*. *Fungal Genet. Biol.* **2015**, 77 95–107.

41. Torriani S.F.; Penselin D.; Knogge W.; Felder M.; Taudien S.; Platzer M.; McDonald B.A.; Brunner P.C. Comparative analysis of mitochondrial genomes from closely related Rhynchosporium species reveals extensive intron invasion. Fungal *Genet. Biol.* **2014**, 62, 34–42.

Preprints (www.preprints.org) | NOT PEER-REVIEWED | Posted: 8 July 2019 doi:10.20944/preprints201907.0119.v1

42. Koszul R.; Malpertuy A.; Frangeul L.; Bouchier C.; Wincker P.; Thierry A.; Duthoy S.; Ferris S.; Hennequin C.; Dujon B B. The complete mitochondrial genome sequence of the pathogenic yeast Candida (Torulopsis) glabrata. *FEBS Lett.* **2003**, 534 39–48.

43. Losada L.; Pakala S.B.; Fedorova N.D.; Joardar V.; Shabalina S.A.; Hostetler J.; Pakala S.M.; Zafar N.; Thomas E.; Rodriguez-Carres M.; Dean R.; Vilgalys R.; Nierman W.C.; Cubeta M.A. Mobile elements and mitochondrial genome expansion in the soil fungus and potato pathogen Rhizoctonia solani AG-3. *FEMS Microbiol. Lett.* **2014**, 352, 165–173.

44. Oh J.; Kong W.S.; Sung G.H. Complete mitochondrial genome of the entomopathogenic fungus *Beauveria pseudobassiana* (Ascomycota, Cordycipitaceae). *Mitochondrial DNA* **2015**, 26, 777–778.

45. Sande W.W. van de. Phylogenetic analysis of the complete mitochondrial genome of *Madurella mycetomatis* confirms its taxonomic position within the order Sordariales. *PLoS One* **2012**, 7, e38654.

46. Funk E.; Adams A.A.; Spotten S.M.; Van Hove R.A.; Whittington K.T.; Keepers K.; Pogoda C.S.; Lendemer J.; Trip E.A.; Kane N.C. The complete mitochondrial genomes of five lichenized fungi in the genus Usnea (Ascomycota: Parmeliaceae). *Mitochondrial DNA Part B* **2018**, 3, 305–308.

47. Sandor S.; Zhang Y.; Xu J. Fungal mitochondrial genomes and genetic polymorphisms. *Appl. Microbiol Biotechnol.* **2018**, 102, 9433–9448

Preprints (www.preprints.org) | NOT PEER-REVIEWED | Posted: 8 July 2019 doi:10.20944/preprints201907.0119.v1